

A novel air-stable n-type organic semiconductor: 4,4'-bis[(6,6'-diphenyl)-2,2-difluoro-1,3,2-dioxaborine] and its application in organic ambipolar field-effect transistors

Yanming Sun,^a Dirk Rohde,^b Yunqi Liu,^{*a} Lijun Wan,^{*b} Ying Wang,^a Weiping Wu,^a Chongan Di,^a Gui Yu^a and Daoben Zhu^{*a}

Received 21st June 2006, Accepted 7th September 2006

First published as an Advance Article on the web 3rd October 2006

DOI: 10.1039/b608840f

Novel air-stable n-type organic field-effect transistors based on 4,4'-bis[(6,6'-diphenyl)-2,2-difluoro-1,3,2-dioxaborine] (DOB) have been fabricated. The devices exhibit a field-effect mobility of $1 \times 10^{-4} \text{ cm}^2 \text{ V}^{-1} \text{ s}^{-1}$, an on/off ratio of 10^4 and a threshold voltage of 8.6 V at room temperature under ambient conditions. Moreover, ambipolar organic field-effect transistors based on DOB and copper phthalocyanine (CuPc) have been fabricated. Two device structures were adopted to investigate their transport properties. When devices were constructed with DOB as the first layer and CuPc as the second layer, they showed typical ambipolar transport properties. However, when the two layers were exchanged, the devices only showed p-channel transport properties. It is probable that CuPc, a bad electron transport material, blocks the electron transport to the DOB layer, leading to the disappearance of electron enhancement.

Introduction

Organic field-effect transistors (OFETs), whose characteristics are modulated by an electrical field, are probably the most prominent constituent of modern microelectronics.¹ They have attracted increasing interest especially in the fields of flexible and low-cost electronic applications, such as low-end display driving circuits, pliable electronic paper, radio-frequency identification tags and smart cards.^{2–9} Among the organic semiconductors, most materials tend to transport holes better than electrons, thus there are more p-type materials, such as the linear acenes and oligothiophenes. For example, for rubrene, a tetraphenyl derivative of tetracene, a field-effect mobility of $15 \text{ cm}^2 \text{ V}^{-1} \text{ s}^{-1}$ has been obtained for a single crystal.¹⁰ Taking pentacene as the benchmark material in organic semiconductors, its mobilities above $1 \text{ cm}^2 \text{ V}^{-1} \text{ s}^{-1}$ have been reported, which are close to the criterion for amorphous silicon (a-Si:H) devices.¹¹ However, on the whole, the number of n-type materials is still limited and their performance has not up to now been satisfactory. Due to this and the fact that high performance n-type semiconductors are important components of p–n junction diodes, ambipolar transistors, and complementary circuits, the development of n-type materials is urgently required.

Ambipolar OFETs are considered to be crucial for the development of complementary circuits with a high degree of robustness, low power dissipation and a good noise margin. The research on these has lately been gaining much attention

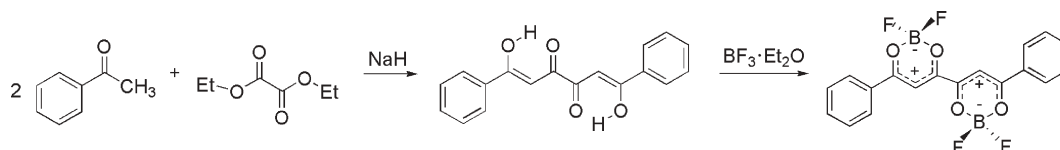
and several research groups have reported work in this field.^{12–21} Due to the intrinsic properties of organic semiconductors, most OFETs only show unipolar properties, and it is normally difficult to obtain ambipolar OFETs characteristics (showing both n- and p-channel properties) in a single layer device structure. Currently, ambipolar devices can be fabricated by several methods, such as employing a blend of two materials,^{12–14} a bilayer organic heterostructure^{15,16} and a low-function metal, to balance the injection of holes and electrons in one layer.¹⁹ While on the one hand the carrier mobilities of these devices are quite low, especially for n-channel transport, on the other hand most of them are unstable under ambient conditions. Despite this, air-stable ambipolar OFETs based on blends of poly(benzobisimidazobenzophenanthroline) and copper phthalocyanine (CuPc),¹⁴ and hexadecafluorophthalocyaninatocopper (F₁₆CuPc) and CuPc have been reported recently.^{20,21} Nevertheless, there are few examples of ambipolar OFETs that are stable in air. This is mainly due to the scarcity of air-stable n-type organic semiconductors, most of them being sensitive to O₂ and H₂O. In this contribution, we have reported an air-stable compound, 4,4'-bis[(6,6'-diphenyl)-2,2-difluoro-1,3,2-dioxaborine] (DOB). Furthermore, ambipolar organic field-effect transistors based on DOB and CuPc have been fabricated and characterized.

Results and discussion

DOB was synthesised by modified methods according to Scheme 1.^{22,23} 1,6-Dihydroxy-1,6-diphenyl-1,5-diene-3,4-dione was obtained under Claisen condensation conditions from acetophenone and oxalic acid diethyl ester in a ratio of two to one. For the complexation, the 1,6-dihydroxy-1,6-diphenyl-1,5-diene-3,4-dione was dissolved in acetic acid. To a boiling solution, an excess of boron trifluoride etherate was added

^aKey Laboratory of Organic Solids, Institute of Chemistry, Chinese Academy of Sciences, Beijing, 100080, People's Republic of China. E-mail: liuyq@mail.iccas.ac.cn

^bKey Laboratory of Molecular Nanostructure and Nanotechnology, Institute of Chemistry, Chinese Academy of Sciences, Beijing, 100080, People's Republic of China. E-mail: wanlijun@mail.iccas.ac.cn



Scheme 1 Synthesis of 4,4'-bis[(6,6'-diphenyl)-2,2-difluoro-1,3,2-dioxaborine] (DOB).

drop-wise. The product was crystallized from the hot solution and then isolated by filtration. Finally, the product was recrystallized from acetic acid.

Due to its high electron affinity,²⁴ the dioxaborine is easy to reduce. From cyclic voltammetric (CV) measurements in acetonitrile, it shows two reversible reduction waves at 0.06 V and -0.44 V *versus* SCE. Therefore, the LUMO level of DOB (about 4.4 eV) can be estimated from its CV results;^{25,26} a value similar to that of $F_{16}CuPc$.²⁷ The latter is an excellent air-stable n-type compound which is well known to us. By comparison, the HOMO level of CuPc is 5.3 eV,¹⁹ which matches well with the work function of Au (5.1 eV), favoring hole injection from the electrode to CuPc. Due to the mismatch in energy levels for DOB, an injection barrier of 0.7 eV for electron injection from Au to DOB is formed. We note that this energy barrier can be overcome by applying a perpendicular gate field according to ref. 12.

In order to investigate the electrical characteristics of DOB, we fabricated a single-layer FET device with a top-contact configuration. A highly n-doped Si wafer covered with thermally oxidized SiO_2 (470 nm) was used as the gate electrode. A 50 nm thick DOB thin film was vacuum-deposited at a pressure of 5×10^{-4} Pa. Fig. 1 shows the plots of the drain current (I_D) *versus* drain-source voltage (V_D) and the drain current *versus* gate voltage (V_G) characteristics for the devices. From the output curves, good linear regions and saturation regions can be seen. Only n-channel activity is observed for the device, indicating electrons are the major charge carriers in the conducting channel. According to the equation below, the mobility in the saturation regime can be calculated.

$$I_D = (W/2L)C_i\mu(V_G - V_T)^2$$

where μ is the field-effect mobility, L and W are channel length and width, respectively, C_i is the insulator capacitance per unit area (10 nF cm^{-2}), and V_T is the extrapolated threshold voltage. From the equation, a mobility of $1 \times 10^{-4} \text{ cm}^2 \text{ V}^{-1} \text{ s}^{-1}$, an on/off ratio about 10^4 , and a threshold voltage of 8.6 V can be obtained with a gate dielectric treated with octadecyltrichlorosilane (OTS) at room temperature. Furthermore, after standing for one week under ambient conditions, the devices show good stability without substantial change in field-effect performance. The mobility only varied from $1 \times 10^{-4} \text{ cm}^2 \text{ V}^{-1} \text{ s}^{-1}$ to $0.79 \times 10^{-4} \text{ cm}^2 \text{ V}^{-1} \text{ s}^{-1}$ and the on/off ratio was almost unchanged. The introduction of the strongly electron-withdrawing fluorine atoms may lower the LUMO level and enhance the stability of the DOB molecules.

The thin films of DOB were investigated by X-ray diffraction in reflection mode. Highly crystalline films were observed, as seen in Fig. 2. The intensity of the first peak is very strong, as is the second peak, indicating that the films possess well-ordered, layered microstructures. From the XRD

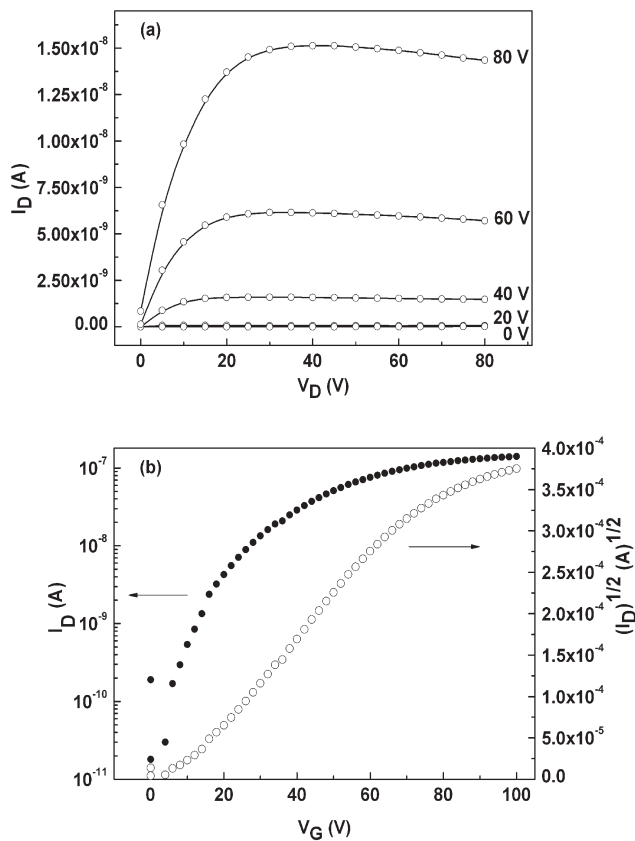


Fig. 1 The electrical characteristics of single-layer DOB FET devices. (a) Drain current *versus* drain-source voltage as a function of gate voltages. (b) The transfer curve at a drain-source voltage of 100 V and the square root of the positive value of the current as a function of the gate voltages.

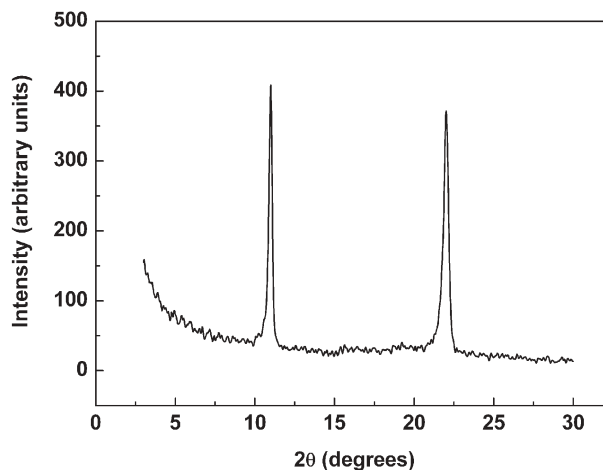


Fig. 2 X-Ray diffraction patterns acquired for an evaporated thin film of DOB.

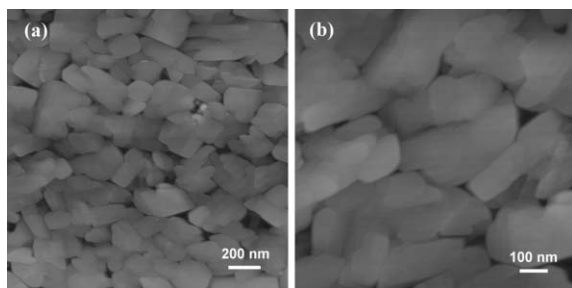


Fig. 3 AFM images of a DOB thin film evaporated on SiO₂ surfaces with OTS treatment at room temperature, with different dimensions for (a) and (b).

data of the thin films, the interplanar d spacings can be calculated. According to the results of the first-layer line, the monolayer thickness is 0.8 nm. The length of the molecule is about 1.6 nm, calculated using the PM3 method. This indicates the molecule has a tilt angle of about 60° from the normal to the substrate. The big tilt angle is not propitious to the transport of charge carriers and as a result, the mobility is moderate. Fig. 3 shows the AFM topographic images of DOB thin films deposited on SiO₂/Si with surfaces treated with OTS at room temperature. Fig. 3a and Fig. 3b are the images of DOB with dimensions of 2 μm × 2 μm and 1 μm × 1 μm, respectively. Small crystal grains with an average diameter of about 200 nm were observed in thin films, and the grains showed terrace-like layered structures. The height of the two layers is approximately 0.8 nm, which corresponds well to the d spacing from the XRD results of thin films of DOB described above.

Employing DOB and CuPc as the n-type and p-type materials, respectively, we have fabricated ambipolar FETs. Two types of device structures were adopted to investigate the ambipolar properties. The schematic diagrams of heterojunction OFETs are given in Fig. 4. DOB thin films 30 nm thick and CuPc thin films 20 nm thick were vacuum-deposited under a base pressure of 5×10^{-4} Pa. Fig. 5 shows the $I_D - V_D$ and $I_D - V_G$ plots of the device with structure (a) (Fig. 4a). Only p-channel FET properties have been found from the output curve. A mobility of $0.033 \text{ cm}^2 \text{ V}^{-1} \text{ s}^{-1}$, an on/off ratio of about 10^5 , and a threshold voltage V_T of -1.2 V can be obtained at a V_D of -60 V . The mobility is among the best displayed for polycrystalline CuPc. Normally, the mobilities of this material are less than or similar to $10^{-2} \text{ cm}^2 \text{ V}^{-1} \text{ s}^{-1}$.^{28–31} The high performance can be attributed to the extra conductive channel at the interface of the heterojunction, which results from the dipolar interface.³² However, for the device with structure (b) (Fig. 4b), typical ambipolar FET properties were found. According to the transfer curve in Fig. 6, the electron and hole mobilities are $2.5 \times 10^{-6} \text{ cm}^2 \text{ V}^{-1} \text{ s}^{-1}$ and $2.2 \times 10^{-4} \text{ cm}^2 \text{ V}^{-1} \text{ s}^{-1}$, respectively. Compared with the single-layer FET devices, the ambipolar mobilities are lower by about one or two orders of magnitude. This result indicates that the concentrations of charge carriers decrease during transport, probably due to the disordered interface effect of the two opposite polar compounds. Further study to optimize the device fabrication conditions is underway.

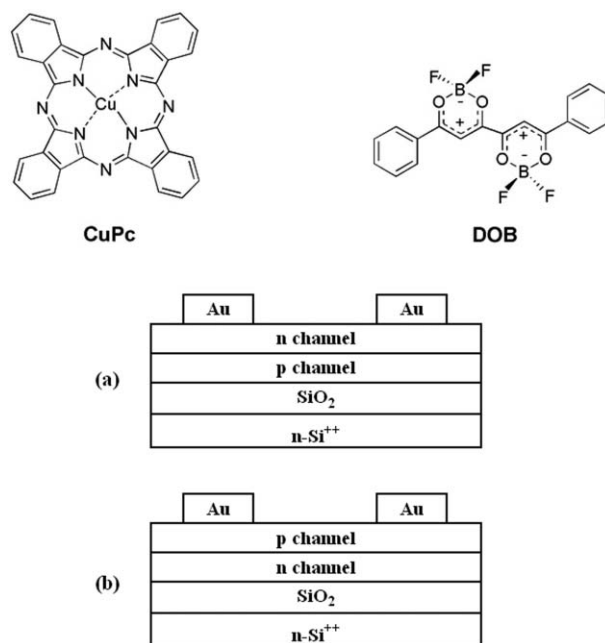


Fig. 4 Schematic diagram of heterojunction OFETs and the chemical structure of CuPc and DOB.

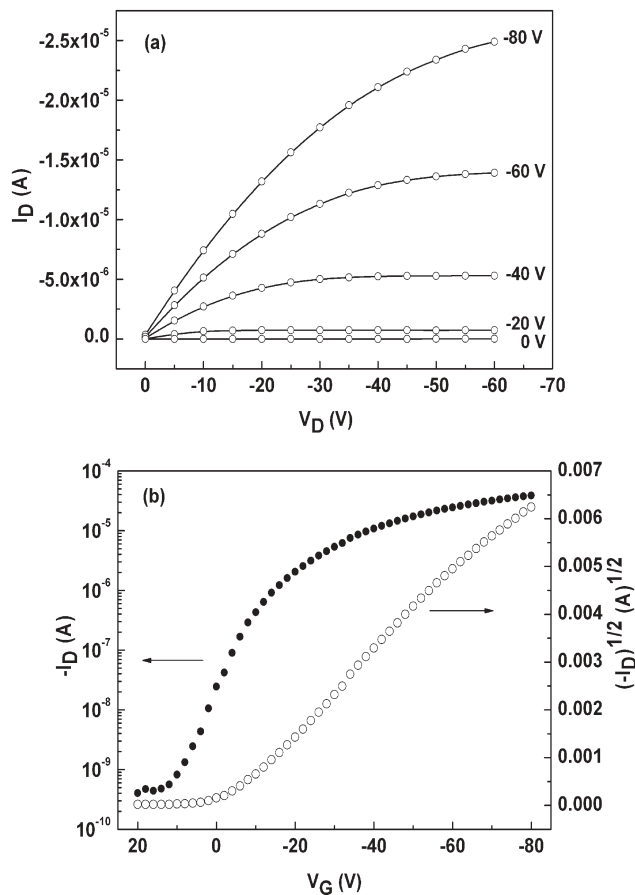


Fig. 5 The electrical characteristics of two-layer FET devices with structure (a) (Fig. 4, DOB thin films on top of CuPc thin films). (a) The output curve at different gate voltages. (b) The transfer curve at a drain-source voltage of -60 V and the square root of the positive value of the current as a function of the gate voltages.

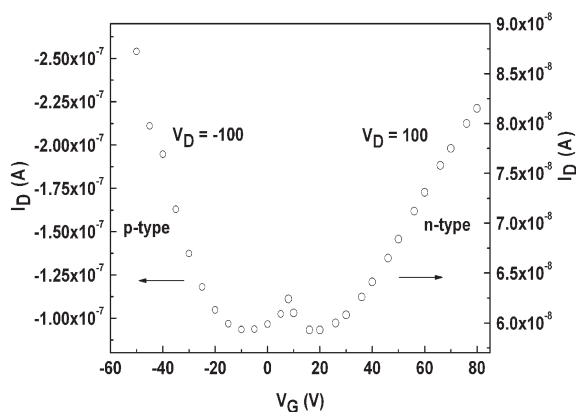


Fig. 6 The transfer characteristics of ambipolar OFETs.

As is common in ambipolar charge carrier transport, when a low bias was applied to the gate electrode, unusual characteristics were seen in the output curve. For p-channel operation, at a low negative V_G and a large negative V_D , I_D increased abruptly due to electron enhancement at the drain electrode. At the same time, holes accumulated at the source electrode and a pn-junction was formed with the two charge carriers, which is responsible for the increased I_D current at low gate voltage.¹² As the V_G increased, the electron enhancement decreased gradually until the appearance of holes and the output curve became normal. For n-channel operation, an accumulation layer of holes was formed near the drain electrode, and an accumulation layer of electrons was formed near the source electrode. With increasingly positive V_G , I_D decreased until the output became normal.

In the above paragraph, we have mentioned that when CuPc thin film is the first layer, it is only a p-channel FET action. The reason why it only shows p-channel performance is discussed below. For structure (a), when a positive bias was applied to the gate, electrons should be induced to the interface between DOB and CuPc. However, because CuPc is a bad electron transport material, it blocks the transport of electrons, even though V_G increases to +100 V. This caused a leakage of electrons and led to the absence of n-channel conduction. Therefore, we only observe p-channel action.

Conclusions

In conclusion, we have fabricated novel air-stable FET devices based on DOB. The devices exhibit a field-effect mobility of $1 \times 10^{-4} \text{ cm}^2 \text{ V}^{-1} \text{ s}^{-1}$ and an on/off ratio of 10^4 at room temperature. Furthermore, employing DOB and CuPc as the n-type and p-type materials respectively, we have also fabricated ambipolar FETs. Two device structures were adopted to investigate the ambipolar properties. The devices with DOB as the first layer and CuPc as the second layer show ambipolar transport properties. However, when CuPc is the first layer and DOB is the second layer, the devices only show p-channel transport properties, which is probably due to the fact that CuPc is a bad electron transport material, resulting in the leakage of electrons and causing the disappearance of electron enhancement.

Experimental

Characterization

Elemental analysis (EA) was carried out using a Carlo Erba model 1160 elemental analyzer. ^1H NMR spectra were recorded on a Bruker DMX 400 spectrometer. Chemical shifts were reported as δ values (ppm) relative to internal tetramethylsilane. X-Ray diffraction of thin films were performed in the reflection mode at 40 kV and 200 mA with $\text{CuK}\alpha$ radiation using a 2 kW Rigaku X-ray diffractometer. AFM images of the thin films were obtained by using a Digital Instruments Nanoscope IIIa in tapping mode under ambient conditions. Cyclic voltammetry measurements were recorded on an Autolab instrument PGSTAT 20. The measurements were performed under N_2 in acetonitrile containing Bu_4NPF_6 as the supporting electrolyte with a scan rate of 0.1 V s^{-1} , using a stationary platinum working electrode, a platinum counter-electrode, and a halogenated silver wire as the reference electrode. Standard redox potentials have been estimated using ferrocene–ferrocenium in acetonitrile as the reference redox system.

Synthesis of 4,4'-bis[(6,6'-diphenyl)-2,2-difluoro-1,3,2-dioxaborine]

A solution of 5 g (0.04 mol) acetophenone and 3 g (0.02 mol) oxalic acid diethyl ester in 300 ml toluene was stirred and heated for 8 hours after the addition of 1 g sodium hydride. After cooling to room temperature, the solution was added to a mixture of water, ice and acetic acid. The organic layer was separated, washed with water, dried over Mg_2SO_4 and concentrated. The product was isolated by filtration (2.7 g), and recrystallized from acetic acid to give 1,6-dihydroxy-1,6-diphenyl-1,5-diene-3,4-dione as a yellow crystalline solid. The yield of the crude product was 50%, mp $187\text{--}189 \text{ }^\circ\text{C}$; ^1H NMR (400 MHz, acetone- d_6) δ_{H} 8.14 (d, 4H), 7.71 (t, 2H), 7.61 (m, 6H); EA: Calc. for $\text{C}_{18}\text{H}_{14}\text{O}_4$ [%]: C 73.4, H 4.7; found [%]: C 73.5, H 4.7.

To a boiling solution of 1.7 g (0.0057 mol) 1,6-dihydroxy-1,6-diphenyl-1,5-diene-3,4-dione in 140 ml acetic acid, 1 ml boron trifluoride etherate adduct was added. After addition, the solution was boiled for a further two minutes. The product crystallized from the hot solution, was isolated by filtration (2.2 g), and was recrystallized from acetic acid followed by sublimation to give bis(6,6'-diphenyl-2,2'-difluoro-1,3,2-dioxaborine) as a yellow crystalline solid. The yield of the crude product was 98%, mp $225 \text{ }^\circ\text{C}$ with decomposition, λ_{abs} (toluene) 414 nm, λ_{fluoro} (toluene) 556 nm; ^1H NMR (400 MHz, CDCl_3) δ_{H} 8.3 (d, 4H), 7.87 (t, 2H), 7.68 (m, 6H); EA: Calc. for $\text{C}_{18}\text{H}_{12}\text{O}_4\text{B}_2\text{F}_4$ [%]: C 55.4, H 3.1, found [%]: C 55.2, H 3.1.

Device fabrication

The devices were fabricated in a top-contact configuration. The substrate is highly *n*-doped Si with a 470 nm layer of thermally oxidized SiO_2 , which served as the gate electrode. Gold was deposited through a shadow mask as the source and drain electrode. The channel length $L = 0.05 \text{ mm}$ and the channel width $W = 3 \text{ mm}$. The characteristics of the OFETs

were obtained at room temperature in air using a Hewlett-Packard (HP) 4140B semiconductor parameter analyzer at different gate voltages.

Acknowledgements

The authors gratefully acknowledge financial support from the National Natural Science Foundation of China (NNSFC), the Major State Basic Research Development Program and the Chinese Academy of Sciences.

References

- 1 G. Horowitz, *Adv. Mater.*, 1998, **10**, 365.
- 2 C. D. Sheraw, L. Zhou, J. R. Huang, D. J. Gundlach, T. N. Jackson, M. G. Kane, I. G. Hill, M. S. Hammond, J. Campi, B. K. Greening, J. Francl and J. West, *Appl. Phys. Lett.*, 2002, **80**, 1088.
- 3 B. Comiskey, J. D. Albert, H. Yoshizawa and J. Jacobson, *Nature*, 1998, **394**, 253.
- 4 B. Crone, A. Dodabalapur, A. Gelperin, L. Torsi, H. E. Katz, A. J. Lovinger and Z. Bao, *Appl. Phys. Lett.*, 2001, **78**, 2229.
- 5 C. J. Drury, C. M. J. Mutsaers, C. M. Hart, M. Matters and D. M. de Leeuw, *Appl. Phys. Lett.*, 1998, **73**, 108.
- 6 G. H. Gelinck, T. C. T. Geuns and D. M. de Leeuw, *Appl. Phys. Lett.*, 2000, **77**, 1487.
- 7 P. Mach, S. J. Rodriguez, R. Nortrup, P. Wiltzius and J. A. Rogers, *Appl. Phys. Lett.*, 2001, **78**, 3592.
- 8 H. E. A. Huitema, G. H. Gelinck, J. B. P. H. van der Putten, K. E. Kuijk, C. Hart, E. Cantatore, P. T. Herwig, A. J. J. M. van Breemen and D. M. de Leeuw, *Nature*, 2001, **414**, 599.
- 9 P. F. Baude, D. A. Ender, M. A. Haase, T. W. Kelley, D. V. Muires and S. D. Thesis, *Appl. Phys. Lett.*, 2003, **82**, 3964.
- 10 V. C. Sundar, J. Zaumseil, V. Podzorov, E. Menard, R. L. Willett, T. Someya, M. E. Gershenson and J. A. Rogers, *Science*, 2004, **303**, 1644.
- 11 Y.-Y. Lin, D. J. Gundlach, S. F. Nelson and T. N. Jackson, *IEEE Electron Device Lett.*, 1997, **18**, 606.
- 12 E. J. Meijer, D. M. De Leeuw, S. Setayesh, E. Van Veenendaal, B.-H. Huisman, P. W. M. Blom, J. C. Hummelen, U. Scherf and T. M. Klapwijk, *Nat. Mater.*, 2003, **2**, 678.
- 13 M. Shkunov, R. Simms, M. Heeney, S. Tierney and I. McCulloch, *Adv. Mater.*, 2005, **17**, 2608.
- 14 A. Babel, J. D. Wind and S. A. Jenekhe, *Adv. Funct. Mater.*, 2004, **14**, 891.
- 15 A. Dodabalapur, H. E. Katz, L. Torsi and R. C. Haddon, *Appl. Phys. Lett.*, 1996, **68**, 1108.
- 16 E. Kuwahara, Y. Kubozono, T. Hosokawa, T. Nagano, K. Masunari and A. Fujiwara, *Appl. Phys. Lett.*, 2004, **85**, 4765.
- 17 T. D. Anthopoulos, D. M. de Leeuw, E. Cantatore, S. Setayesh, E. J. Meijer, C. Tanase, J. C. Hummelen and P. W. M. Blom, *Appl. Phys. Lett.*, 2004, **85**, 4205.
- 18 Th. B. Singh, F. Meghdadi, S. Günes, N. Marjanovic, G. Horowitz, P. Lang, S. Bauer and N. S. Sariciftci, *Adv. Mater.*, 2005, **17**, 2315.
- 19 T. Yasuda and T. Tsutsui, *Chem. Phys. Lett.*, 2005, **402**, 395.
- 20 J. Wang, H. Wang, X. Yan, H. Huang and D. Yan, *Chem. Phys. Lett.*, 2005, **407**, 87.
- 21 R. Ye, M. Baba, Y. Oishi, K. Mori and K. Suzuki, *Appl. Phys. Lett.*, 2005, **86**, 253505.
- 22 A. Hunze, A. Kanitz, H. Hartmann and D. Rohde, WO 02/065600; Chem. Abstr., 2003, **137**, 187010.
- 23 J. M. Halm and J. H. DeLorme, *Photogr. Sci. Eng.*, 1979, **23**, 252.
- 24 J. Fabian and H. Hartmann, *J. Phys. Org. Chem.*, 2004, **17**, 359.
- 25 Z. Chen, M. G. Debije, T. Debaerdemaeker, P. Osswald and F. Würthner, *ChemPhysChem*, 2004, **5**, 137.
- 26 A. Facchetti, M.-H. Yoon, C. L. Stern, G. R. Hutchison, M. A. Ratner and T. J. Marks, *J. Am. Chem. Soc.*, 2004, **126**, 13480.
- 27 C. F. Shen and A. Kahn, *J. Appl. Phys.*, 2001, **90**, 4549.
- 28 K. Xiao, Y. Q. Liu, G. Yu and D. B. Zhu, *Synth. Met.*, 2003, **137**, 991.
- 29 K. Xiao, Y. Q. Liu, Y. Guo, G. Yu, L. Wan and D. B. Zhu, *Appl. Phys. A: Solid Surf.*, 2005, **80**, 1541.
- 30 Z. Bao, A. J. Lovinger and A. Dodabalapur, *Adv. Mater.*, 1997, **9**, 42.
- 31 Z. Bao, A. J. Lovinger and A. Dodabalapur, *Appl. Phys. Lett.*, 1996, **69**, 3066.
- 32 J. Wang, H. B. Wang, X. J. Yan, H. C. Huang and D. H. Yan, *Appl. Phys. Lett.*, 2005, **87**, 093507.